Single phase positive output super-lift luo converter fed high power LED lamp with unity power factor and reduced source current harmonics

J. GNANAVADIVEL[a,*], N. SENTHIL KUMAR[a], C. N. NAGA PRIYA[b], S. T. JAYA CHRISTA[a], K. S. KRISHNA VENI[a]

[a]*Electrical and Electronics Engineering Department, Mepco Schlenk Engineering College, Sivakasi, Tamilnadu, India*

[b]*Electrical and Electronics Engineering Department, Sri Vidya College of Engineering and Technology, Virudhunagar, Tamilnadu, India*

In this paper, a proposed single phase positive output super-lift Luo converter fed high power LED lamp for industrial lighting with improved power quality at input side has been presented. This converter boosts up the input voltage with high gain ratio. The proposed converter operates in continuous conduction mode. The design and simulation of 100 W LED driver is carried out in Matlab/Simulink platform with constant load voltage of 48V. Closed loop control incorporates outer voltage control and inner current control. A novel Adaptive Neuro Fuzzy Inference System (ANFIS) controller is proposed for voltage control, which tunes the Proportional and Integral (PI) parameters and Hysteresis controller is used in current loop. From the simulation results, it is found that the proposed LED lamp driver with controller combination gives the best result with a low total harmonic distortion and unity power factor with no peak-over shoot at rated condition. The proposed system is implemented in real time in order to validate the performance of the proposed system over a wide range of output power with improved power quality at AC mains using Xilinx Spartan-6 XC6SLX25 FPGA board.

(Received December 10, 2015; accepted November 25, 2016)

Keywords: Adaptive Neuro Fuzzy Inference System, PI controller, Positive output super-lift Luo Converter, LED, Input Power Factor, Total Harmonic Distortion

1. Introduction

Now-a-days, light emitting diode lamps are gaining popularity in both industrial and domestic usage. It can be used in many applications even from street lights to car head lights. Improvement in the lighting technology from the past few years result in plenty of advantages such as high luminous efficiency, long life, low power consumption, environment friendly because there is less mercury contents, easily dimmable, low maintenance, flicker less start, robust in structure and least affected by vibrations[1]-[6]. Even though LED lamp offers many merits, it also has some demerits such as generation of harmonics in the input AC side and low input power factor because of switching devices used in the LED driver. LED lighting module consists of two major parts: LED driver and LED module. In many research articles they focused on the development of LED lamps, lighting control and illumination on the work surface [7] - [12]. Only few research papers so far published focus on the improvement of power quality in the AC supply side of the LED lamp driver.

In general, an AC/DC converter uses as a diode bridge rectifier and a large value of capacitor to obtain smooth dc link voltage. This type of LED driver introduces highly distorted source current which results in high value of total harmonic distortion and very low input power factor. To maintain the power quality, standards of the harmonic regulation such as IEC 61000-3-2 class C enacted to limit the source current harmonics and to guarantee input power factor of 0.9 at least.

Therefore, some steps have to be taken in order to improve the power factor and the best method to accomplish is to use power factor correction (PFC) converters as a LED driver circuit. The commonly used power factor correction converters are buck, boost, buck-boost, Cuk, Sepic , Zeta and flyback converters along with diode bridge rectifier[13]-[17] and these converters can operate in continuous conduction mode or discontinuous conduction mode to achieve better power quality in the supply side. To reduce the switching stress and conduction losses, Boost-interleaved buck-boost converter is employed in [13], and it results in THD of nearly 4.6% which is within in the limit of IEC and IEEE standards.

Fly back buck-boost converter [14] is introduced for low power applications with voltage follower approach in order to get low THD (4.8%) and improved power factor. (0.992). PFC Cuk converter is used with current multiplier approach to maintain harmonics ranging from 3.85% to 7.42% with variation in the DC link voltage[15]. To reduce the conduction losses, SEPIC converter is employed in [16]. Isolated zeta converter is used for PFC correction in [17]. With this system, source current harmonics gets reduced to 3.7% and also the power factor gets improved in the front end. Three level boost converter

and low frequency PWM converter are used for PFC in LED drive applications [18], [19].

Bridgeless topology was introduced, in order to reduce the conduction losses possessed by the conventional rectifier topologies. Bridgeless Sepic converter is employed at the front end to improve the power quality indices which results in further decline in THD in the order of 2.16% [20]. The harmonic distortions are only 2.12% in case of bridgeless Zeta converter [21]. In [22] bridgeless Luo converter topology is presented in order to improve the power factor and the harmonics in this system is found to be 4%. Even though, the above mentioned topologies operate with minimized conduction losses, they account for high switching losses due to increased number of components. Also, for these systems the voltage transfer gain is low and ripple content in output voltage is high.

In this paper, a single phase positive output super-lift Luo converter is considered to improve the quality of power and to mitigate various power quality issues. Super-lift Luo converter is extensively used because of its excellent response even during load variations , supply voltage fluctuations and the voltage lift technique is used in many high voltage gain converters in which the output voltage increases stage by stage progressively[23]-[27]. Though the gain ratio increases in geometric progression on stage-by-stage in super-lift technique, they are quite complex to design. To overcome this disadvantage, an efficient positive output super-lift Luo converter is introduced to enhance the voltage transfer gain in power law terms [28].

In regard to the controller part, generally PI controller is used which offers several advantages such as stability even for large line and load variations, reduced steady state error, robustness, good dynamic response and easy implementation[29]. Though PI controller posses lot of advantages, the main challenge is involved in the design of current loop. Because, it requires an accurate mathematical model of the plant otherwise its performance during load disturbance and parameter variation are not satisfactory [30]. Whereas Hysteresis current controller does not require any accurate mathematical modeling when the controller is being designed [31]. Also this technique has an advantage of yielding instantaneous current control, which results in a very fast response and increased switch reliability.

The hysteresis current control method is widely used because of its ease in implementation and quick current controllability [32]. The hysteresis band current control is robust and it provides excellent dynamics and fastest control response with minimum hardware. The voltage controller performance is further improved by designing good input and output membership function of the fuzzy logic controller. Traditional ways for designing controllers of DC/DC converters are based on small signal model and the validation of small signal model is limited by changes in the operation point [33].

Among the various techniques of artificial intelligence, fuzzy logic is the most popular one for controlling a system. An intelligent controller, with proper design, works very well even with an approximate model of the system. The adaptive-fuzzy controller is used to improve the system's dynamic response and the parameters of PI controllers are adjusted online. The conventional PI controller produces constant K_p, K_i values which need to be changed during continuous system variations [34]. The intelligent agent based Adaptive Neuro-Fuzzy Inference System (ANFIS) was developed to make system stable even under external disturbances [35] - [38].

The main objective of the proposed system is to design a single phase positive output super-lift Luo converter based LED driver with high power factor and reduced THD even under source voltage and load fluctuations. Fuzzy supervised ANFIS controller is used to tune the PI parameters. This properly tuned system makes it to offer plenty of advantages such as regulated output voltage with very low overshoot, less settling time, very low harmonics and unity power factor. The proposed work is rationalised by comparing the results obtained in simulation with the PI-hysteresis and fuzzy tuned PI-hysteresis.

2. Proposed topology of LED driver

Fig. 1 shows the circuit diagram of single phase positive output super-lift Luo converter. The proposed system consists of a single phase diode bridge rectifier, inductors (filter and boost), fast recovery diodes, DC capacitors and switching component. The proposed system is designed properly and their performances are investigated for a wide range of variations in load side and supply side.

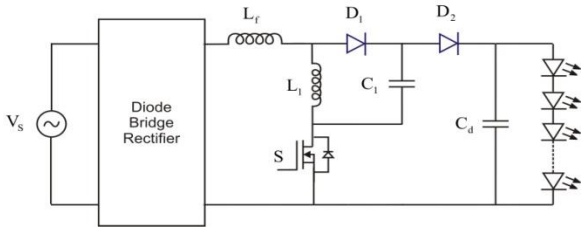

Fig. 1. Proposed Single phase positive output super-lift Luo converter based LED driver

2.1 Modes of operation of proposed LED driver circuit

Based on the switching action of the proposed LED driver circuit, the modes of operation can be classified into two types and they are given below.

Mode 1:

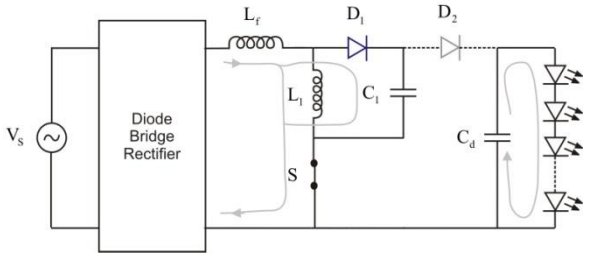

Fig. 2 Mode 1 operation

During mode 1 operation, the switch S is considered to be in ON state thereby, capacitor C_1 gets charged to V_s. The current i_{L1} flowing through inductor increases with voltage V_s. The input current i_s will be equal to $i_{L1} + i\ c_1$. The mode 1 operation is depicted clearly through Fig.2. The characteristic equation during mode 1 operation are given below,

$$\left|v_s\right| = L_1 \frac{di}{dt} = v_{c_1} \tag{1}$$

$$C_d \frac{dv_0}{dt} + \frac{v_0}{R_{lamp}} = 0 \tag{2}$$

Mode 2:

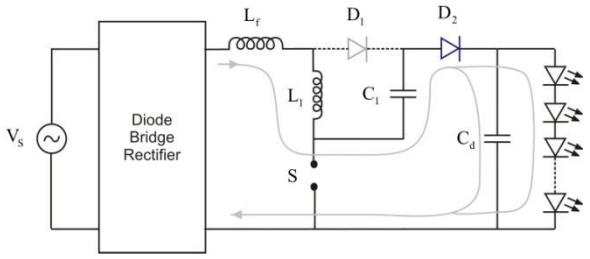

Fig. 3. Mode 2 operation

Fig.3 clearly shows the mode 2 operation of single phase positive output super-lift Luo converter based LED drive. During mode 2 operation, switch S is considered to be in OFF state, diode D_1 is reversed biased and D_2 becomes forward biased. During mode 2 operation, input current will be equal to i_{L1} (=i_{co}).The characteristic equations are,

$$\left|v_s\right| = L_1 \frac{di_{L_1}}{dt} + v_{c_1} + v_0 \tag{3}$$

$$C_d \frac{dv_0}{dt} + \frac{v_0}{R_{lamp}} = i_{L_1} \tag{4}$$

3. Design of the proposed high power factor LED Driver

The following assumptions are considered to design the proposed high power factor LED driver circuit.

1. All the device components of the proposed LED driver circuit are ideal one.
2. Under normal operating condition Light Emitting Diode behaves as a resistor.

The inductance L_1 is determined by the peak-to-peak ripple current ΔI_{L_1}. Therefore, the inductance L_1 can be represented as,

$$L_1 = \frac{V_o - 2V_{in}}{\Delta I_{L_1} f} \tag{5}$$

The capacitor value can be calculated by the formula given below,

$$C_1 = C_d = \frac{(1-k)V_0}{f R_{lamp} \Delta V_0} \tag{6}$$

The output voltage equation of proposed LED driver is,

$$V_0 = \frac{2-k}{1-k} V_{in} \tag{7}$$

The voltage across the diode bridge rectifier is given by,

$$V_{in} = \frac{2(V_m)}{3.14} \tag{8}$$

where

k is the duty cycle

V_o is the DC output voltage

V_m is the peak value of the input voltage

V_s is the supply voltage

V_{in} is the voltage across the diode bridge rectifier

ΔI_{L_1} is the peak to peak ripple inductor current(5% of inductor current I_{L_1})

f is the switching frequency

ΔV_o is the output ripple voltage (2% of output voltage V_o)

R_{lamp} is the LED lamp resistance under normal operating condition

By using the design equations, the values of circuit components are calculated and they are listed in Table 1.

Table 1. Design parameters of proposed LED driver.

Parameter	Specification
Supply voltage (V_s)	20 V
LED lamp voltage(V_{Lamp})	48 V
LED lamp power(P_o)	100 W
Supply frequency(f_L)	50 Hz
Inductor L_f	1.4 mH
Inductor L_1	1.6 mH
Capacitor C_1= C_d	2000 µF

4. Block diagram of the proposed controller

The control structure of the proposed single phase positive output super-lift Luo converter based LED driver is shown in Fig.4. The proposed LED driver control system consists of voltage controller, power estimator, phase locked loop and current controller. The output voltage is sensed and it is compared with the reference voltage. After comparison, the obtained error signal is fed to the voltage controller. Then, the output signal from the power estimator block and the control signal from the voltage controller are added. The obtained value is then multiplied with the PLL output to get reference inductor current. The rectified sinusoidal signal is multiplied by the amplitude of command current to form the reference inductor current. The reference inductor current is expressed as,

$$i_{ref} = \left(\frac{v_0 i_0}{v_{s.peak}} + K_p v_{err} + K_i \sum v_{err} \right) \sin \omega t \quad (9)$$

$$v_{err} = v_{ref} - v_0 \quad (10)$$

where, K_p–Proportional gain, K_i-Integral gain, V_{ref} - reference voltage, V_o- output voltage

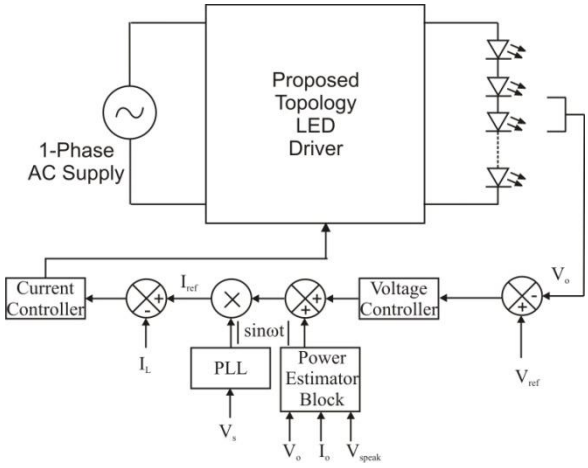

Fig. 4. Control diagram of the proposed single phase positive output super-lift Luo converter based LED driver

The reference inductor current is then compared with the actual inductor current and fed into the inner current loop controller. For voltage control, ANFIS tuned PI is proposed and for current control, hysteresis control generates PWM signal, to maintain proper illumination of LED modules. The power switch 'S' is operating at 10kHz frequency.

5. ANFIS tuned PI controller for high power factor LED driver

The motive behind the design of ANFIS tuned PI controller is to achieve the power quality indices such as reduction in source side harmonics, unity power factor and the load side parameters like minimum settling time and rise time with no peak overshoot. The PI parameters are tuned online using ANFIS controller to improve the system performance such as high input power factor, less harmonic distortion.

ANFIS tuned PI controller needs no separate mathematical modelling of the system similar to Fuzzy logic controller. Here, the data to be loaded is trained again and again according to system response to get zero error from the controller so as to produce perfect results both at input side and output side of the converter. Fig.5 shows the block diagram of ANFIS tuned PI controller for LED driver. The control signal from ANFIS controller is given to the PI controller so that it tunes the PI parameters.

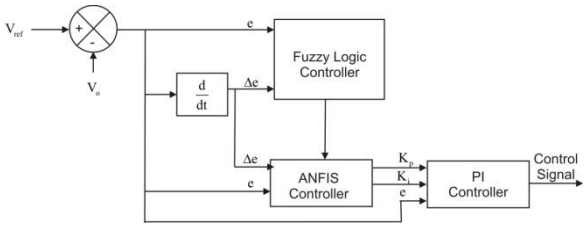

Fig. 5. Block diagram of ANFIS tuned PI controller for LED driver

The structure of the ANFIS network is composed of set of units and connections arranged in network layers from layer1 to layer5 as shown in Fig. 6. ANFIS controller contains four important blocks such as fuzzification, knowledge base, normalisation of fuzzy rules and defuzzification.

Layer 1: It consists of input variables in fuzzy form which has triangular or bell shaped membership functions.

Layer 2: It is the membership layer and it checks for the weights of each membership functions. It receives the input values from the first layer and based on membership functions; represent the fuzzy sets of the respective input variables.

Layer 3: It is called as rule layer and it receives input from the previous layer. Each neuron in this layer performs the pre-condition matching of the fuzzy rules. This layer computes the activation level of each rule and the number of layers equals to the number of fuzzy rules. Each node in this layer calculates the weights which will be normalized.

Layer 4: It is the defuzzification layer which provides the output values resulting from the inference of rules.

Layer 5: It is called as the output layer which sums up all the inputs coming from layer4 and transforms the fuzzy classification results into a crisp value.

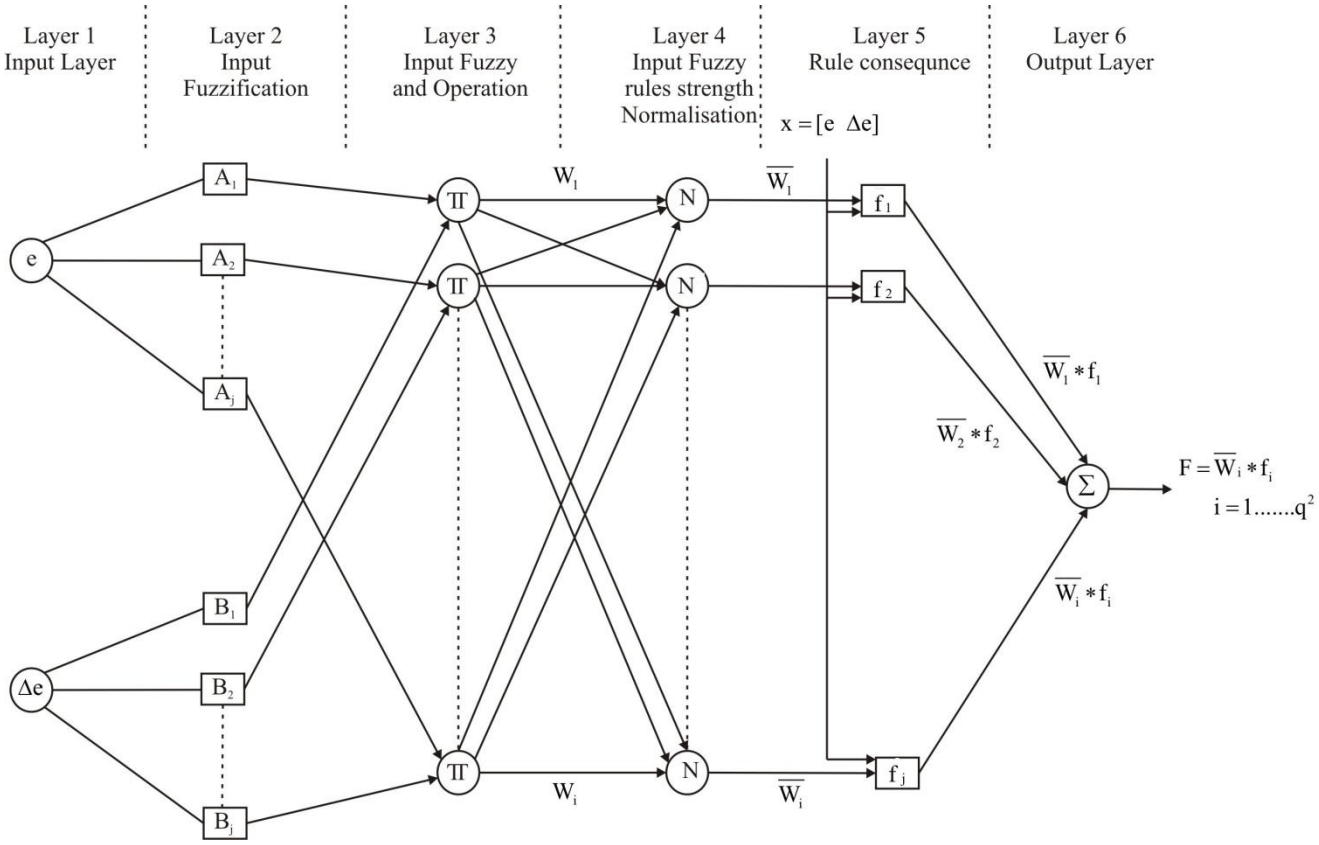

Fig. 6 Layers in ANFIS structure

The IF-THEN rules used are given below.

Rule 1: If e is A_1 and Δe is B_1 then

$$f_1 = P_1 \times e + R_1 \times \Delta e + S_1$$

Rule 2: If e is A_2 and Δe is B_2 then

$$f_2 = P_2 \times e + R_2 \times \Delta e + S_2$$

Rule i-1: If e is A_{i-1} and Δe is B_{i-1} then

$$f_{i-1} = P_{i-1} \times e + R_{i-1} \times \Delta e + S_{i-1}$$

Rule i : If e is A_j and Δe is B_j then

$$f_i = P_i \times e + R_i \times \Delta e + S_i$$

where,

$$e = V_{ref} - V_o$$

$$\Delta e = \frac{d(V_{ref} - V_o)}{dt}$$

A and B are the input variables of the fuzzy membership function, e and Δe are error and change in error and q is the number of membership functions for the fuzzy inputs e and Δe. f_i is the linear consequent function defined in terms of inputs e and Δe. P_i, R_i and S_i are consequent parameters of an ANFIS fuzzy model. Same layer nodes of an ANFIS model have similar functions.

6. Simulation results and analysis of single phase positive output super-lift Luo converter based LED driver with ANFIS tuned PI voltage controller and hysteresis current controller

Fig. 7 shows the simulation diagram of single phase positive output super-lift Luo converter based LED driver with ANFIS tuned PI voltage and hysteresis current controller. The error and change in error are fed as inputs to ANFIS voltage controller. Here ANFIS voltage controller is designed to produce two control signals which are tuned by it with respect to the variations of the system. The tuned values from the controller are multiplied with the error signal and are added. Then the resultant signal is added with the output from the power estimation block and then multiplied with $|\sin \omega t|$ to generate reference inductor current signal. The actual inductor current is compared with the reference signal and given to hysteresis current controller which limits the signal in the band limit of 0.001.

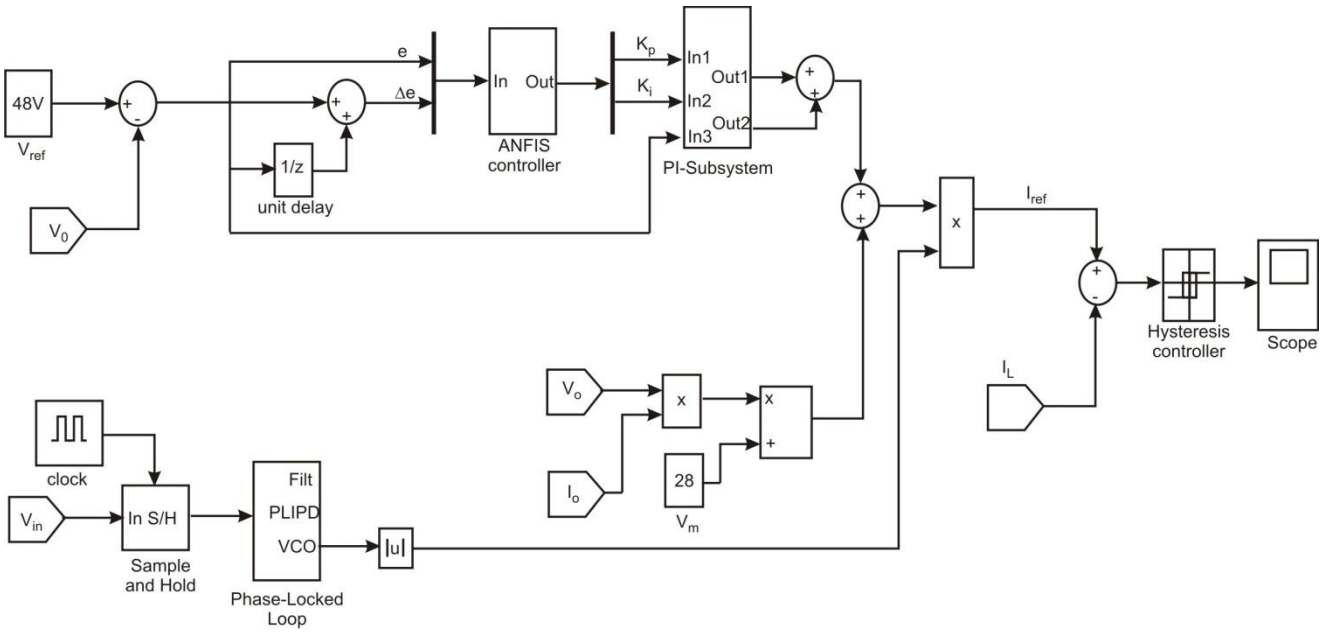

Fig. 7. Simulation diagram of single phase positive output super-lift Luo converter based LED driver with ANFIS tuned PI voltage controller and hysteresis current Controller

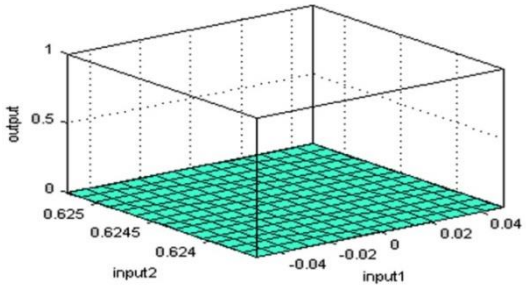

(a)

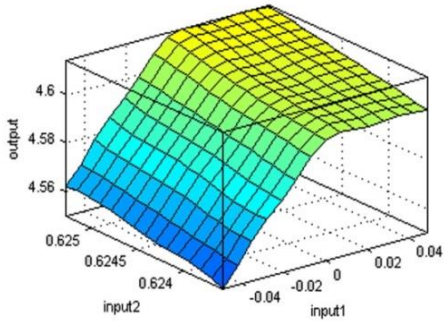

(b)

Fig. 8. a) Initial Rule base (b) Final rule base

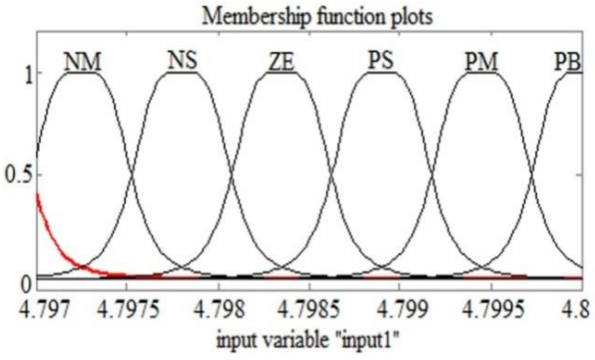

(a)

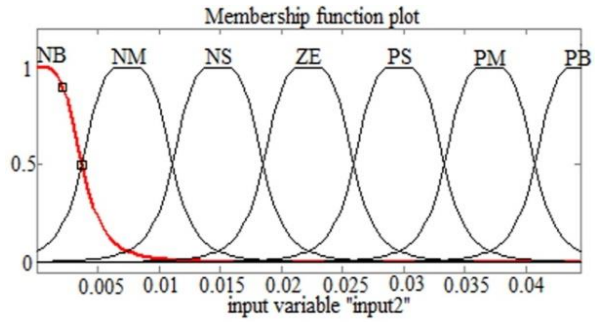

(b)

Fig. 9. Membership function for (a) input 1 (error) (b) input 2(change in error)

Fig.8 shows the rule base model obtained before and after training the data into the ANFIS respectively.

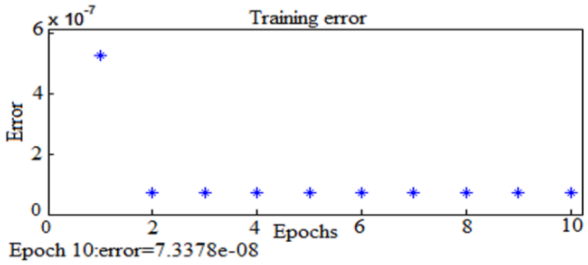

(a)

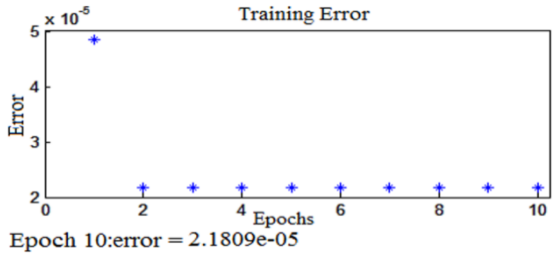

(b)

Fig. 10. Training error Vs Epochs for (a) K_p (b) K_i

Fig. 9 (a) and (b) show the membership functions of input error and change in error respectively after training the data. Fig. 10 (a) and (b) show the training of K_p and K_i values using Neuro-Fuzzy system. The values are trained up to 10 Epochs and the error value is minimised to a very low value which is shown in the Fig. 10.

Fig. 11 shows the layer description of ANFIS obtained during the training of data in ANFIS. In each iterations, two sequences of operations occur; they are forward pass and a backward pass sequence. During forward pass, after an input data is processed, the node outputs are updated layer by layer until, layer 4 is reached. This process is repeated for all training input–output datasets and then, the consequent parameters are identified by least square estimation. In backward pass, the derivative of the error signals with respect to each node propagates from the output end towards the input end.

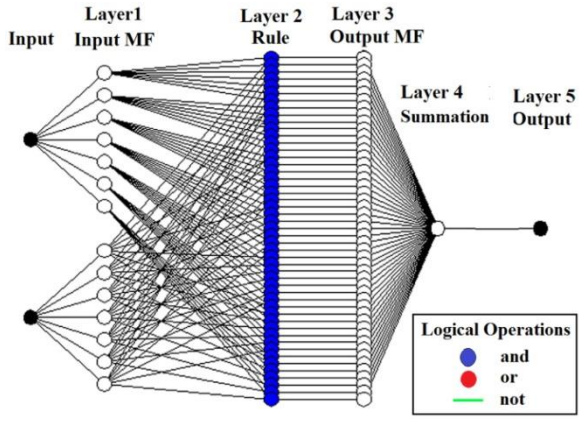

Fig. 11. Layers in ANFIS

Then the gradient vector is accumulated for each input–output training dataset. At the end of the backward pass for all training datasets, the parameters are updated by gradient descent method. Once updating of premise and consequent parameters are completed, proper sets of membership function and rule base are selected for fuzzy inference system. After proper rules are selected and fired, the control signal required to obtain the optimal output is generated. To train the ANFIS controller, the network is trained using MATLAB Simulink tool box. The desired output is trained using the function 'ANFIS' in the MATLAB toolbox. From the training, a fuzzy inference system with adjusted membership function has been obtained.

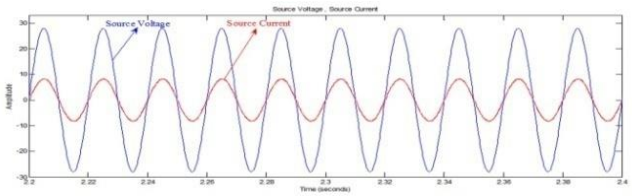

(a)

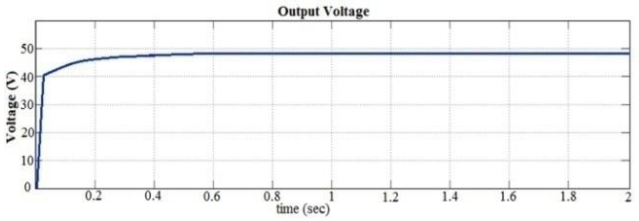

(b)

Fig. 12. (a) Input voltage and input current waveforms (b) Output voltage waveform for ANFIS tuned PI voltage and hysteresis current controller for proposed LED lamp driver at rated lamp power

Fig. 12 (a) shows the input voltage and input current waveforms which are in phase with each other gives unity power factor and the source current distortion is reduced. Fig. 12 (b) shows the output voltage waveform for ANFIS tuned PI voltage and hysteresis current controller and it is observed that there is no peak overshoot and the settling time is 0.55sec.

Fig. 13 (a) shows the FFT analysis of ANFIS tuned PI voltage and hysteresis current controller and THD is reduced to 0.44% during rated LED lamp load condition. Fig. 13 (b) shows the FFT analysis at 10% of LED lamp load with a THD of 1.87% for ANFIS tuned PI voltage and hysteresis current controller.

From the Table 2, it is observed that the output voltage is regulated and maintained constant at 48 V, input power factor is close to unity and source current harmonics reduces from 1.87% to 0.44% for a variation of load from 10% to 100%. It is observed that even under load variations the THD value lies within 5% for ANFIS tuned PI voltage and Hysteresis current controller.

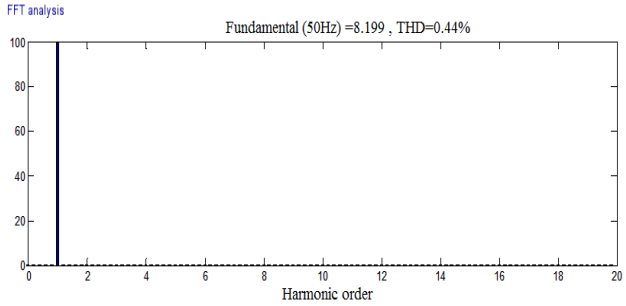

(a)

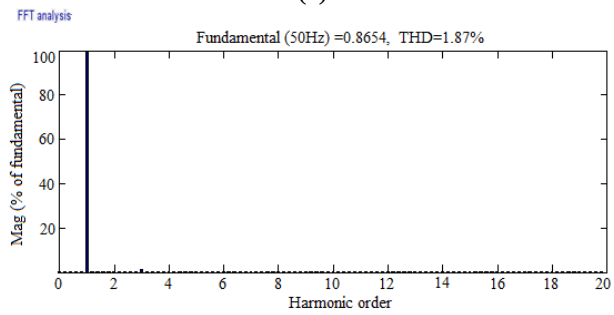

(b)

Fig. 13. (a) FFT analysis at 100% of LED lamp load power (b) FFT analysis at 10% of LED lamp load power for ANFIS tuned PI voltage and hysteresis current controller

Table 2. Performance analysis of single phase positive output super-lift Luo converter based LED driver for ANFIS tuned PI voltage and hysteresis current controller under load variations

LED lamp load power(W)	Output voltage (V)	Input power factor	Source current THD (%)	Source current (A)
100	48	1	0.44	5.797
90	48	1	0.49	5.193
80	48	1	0.51	4.622
70	48	1	0.53	4.013
60	48	1	0.66	3.471
50	48	1	0.76	2.894
40	48	1	0.85	2.324
30	48	0.9999	0.93	1.761
20	48	0.9999	1.17	1.182
10	48	0.9926	1.87	0.611

Table 3. Performance analysis of single phase positive output super-lift Luo converter based LED lamp driver for ANFIS tuned PI voltage and hysteresis current control under supply voltage variations

Supply voltage (V)	Output voltage (V)	Input power factor	Source current THD(%)	Source Current (A)
13	48	0.9979	2.79	10.39
15	48	0.9981	1.97	8.025
20	48	1	0.44	5.797
25	48	0.9999	0.96	4.472
30	48	0.9997	1.24	3.669
35	48	0.9996	1.40	3.125

Table 3 shows the performance analysis of single phase positive output super-lift Luo converter based LED lamp drive under supply voltage variations. The THD value decreases from 2.79% to 0.44% for supply voltage variations from 13V to 35V. It is also observed that the THD value is less than 5% for a wide variation in supply voltage.

Table 4. Source current harmonics for various controllers for a wide variation in LED lamp load power

LED lamp load power(W)	Source current THD (%)		
	PI -Hys	Fuzzy tuned PI- Hys	ANFIS tuned PI - Hys
100	2.72	1.21	0.44
90	3.19	1.46	0.49
80	3.28	1.58	0.51
70	3.54	1.72	0.53
60	3.72	1.91	0.66
50	5.61	2.24	0.76
40	6.21	2.63	0.85
30	7.65	3.75	0.93
20	8.78	4.96	1.17
10	19.6	7.94	1.87

Table 4 shows the comparison of source current harmonics obtained by varying the load from 10% to 100% for various controller combinations. For PI voltage and hysteresis current controller, the THD reduces from 19.6% to 2.72%. For fuzzy tuned PI voltage and hysteresis current controller, the THD decreases from 7.94% to 1.21%. Then to improve the response further, ANFIS tuned PI voltage controller and hysteresis current controller is employed. From the Table 4, it is evident that the ANFIS tuned PI voltage and hysteresis current controller combination gives the best result of 1.87% to 0.44% THD, even for a wide range of load variations.

Table 5. Power factor for various controllers for a wide variation in LED lamp load power

LED lamp load power(W)	Power factor		
	PI-Hys	Fuzzy tuned PI -Hys	ANFIS tuned PI-Hys
100	0.9995	0.9999	1
90	0.9992	0.9998	1
80	0.9991	0.9998	1
70	0.9990	0.9997	1
60	0.9988	0.9996	1
50	0.9983	0.9995	1
40	0.9976	0.9993	1
30	0.9959	0.9989	0.9999
20	0.9910	0.9972	0.9999
10	0.9706	0.9919	0.9926

Table 5 gives the comparison of power factor obtained by varying the LED lamp load power from 10% to 100% for various controller combinations. With PI voltage and hysteresis current controller, the power factor value increases from 0.9706 to 0.9995. Fuzzy tuned PI voltage and hysteresis current controller gives a power factor value of 0.9919 for 10% load and 0.9999 for rated load. To improve the system response ANFIS tuned PI voltage and hysteresis current controller combination is employed and an increase in power factor from 0.9926 to 1 is obtained for an increase in load from 10% to 100%.

Table 6. Source current harmonics for various controllers with a wide variation in supply voltage for proposed LED driver

Source voltage (V)	Source current THD (%)		
	PI-Hys	Fuzzy tuned PI -Hys	ANFIS tuned PI - Hys
15	6.60	2.20	1.97
20	2.72	1.21	0.44
25	1.54	1.99	0.96
30	2.42	2.57	1.24
35	3.14	2.64	1.40

Table 6 shows the comparison of source current harmonics by varying the supply voltage from 15V to 35V below and above the rated input voltage (20V). With the PI voltage and hysteresis current controller, the harmonics decreases from 6.60% to 1.54%. For fuzzy tuned PI voltage and hysteresis current controller, the THD value decreases from 2.64% to 1.2%. To improve the system performance further, the ANFIS tuned PI voltage controller is used at voltage side with hysteresis controller at current side. From the Table 6, it is evident that, the proposed controller for LED driver gives the best result with a decrease in THD from 1.97% to 0.44%.

Table 7. Power factor for various controllers with a wide variation in supply voltage for proposed LED driver

Source voltage (V)	Power factor		
	PI-Hys	Fuzzy tuned PI -Hys	ANFIS tuned PI - Hys
15	0.9966	0.9996	0.9997
20	0.9995	0.9999	1
25	0.9991	0.9997	0.9999
30	0.9990	0.9996	0.9998
35	0.9986	0.9995	0.9997

By varying the supply voltage from 15V to 35V, the power factor is noted for various controller combinations and is tabulated in Table 7. The power factor value increases from 0.9966 to 0.9995 for PI voltage and hysteresis current controller. With fuzzy tuned PI voltage and hysteresis current controller, the power factor value is improved from 0.9995 to 0.9999. Finally ANFIS tuned PI voltage controller with hysteresis current controller is devised to improve the overall system performance. From the Table 7, it can be found that for ANFIS tuned PI voltage and hysteresis current controller, the power factor value increases from 0.9997 to 1.

7. Experimental results of proposed high power factor LED driver

To verify the validity of the proposed ANFIS-tuned PI voltage controller and hysteresis current controller, a single-phase POSLLUO converter based LED driver has been built and tested in the laboratory. It is shown Fig. 14. The power switching devices and various components of the prototype include an MUR360 input rectifier bridge, IRF250 power MOSFET switch, a 1.6mH boost inductor, a 2000 µF output filter capacitor, an FPGA Spartan-6 controller, an HCPL-7840 voltage sensor, a WCS 2705 hall effect current sensor and a LED panel.

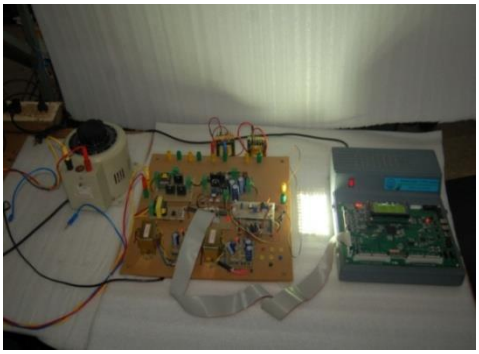

Fig. 14. Hardware setup of proposed LED driver

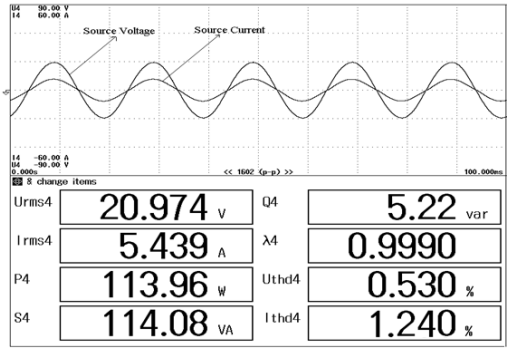

Fig.15a. Experimental input voltage and input current waveforms at rated power with ANFIS tuned PI voltage controller and hysteresis current controller for LED driver

Fig. 15a shows the experimental waveforms of input voltage and input current for rated lamp load power with the ANFIS tuned PI voltage controller and the hysteresis current controller for LED driver. The input power factor and input current THD are measured with the power quality analyzer shown in Fig. 15a. From Fig. 15 a, the input power factor is 0.9990 and the input current THD is 1.240% for the proposed LED driver.

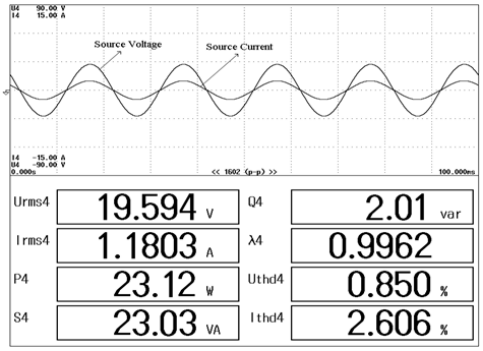

Fig.15b. Experimental input voltage and input current waveforms at 20% of load power with ANFIS tuned PI voltage controller and hysteresis current controller for LED driver

Fig. 15b shows the experimental waveforms of input voltage and input current for 20% of lamp load power with the ANFIS tuned PI voltage controller and the hysteresis current controller for LED driver. The input power factor and input current THD are measured with the power quality analyzer shown in Fig. 15b. From Fig. 15 b, the input power factor is 0.9981 and the THD is 2.606% for the proposed LED driver.

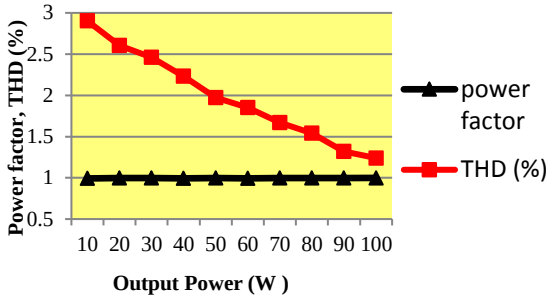

Fig. 15 c. Experimental result for ANFIS tuned PI – hysteresis controller of proposed LED driver

Fig. 15 c depicts the practical readings of the proposed high power factor LED driver with the variation in load.

8. Performance analysis of conventional boost converter with proposed LED driver

The performance of the conventional boost LED driver and proposed LED drive in terms of the obtained input current THD and input PF at the supply mains with output power is evaluated as shown in Fig.16 a and 16 b respectively. ANFIS tuned PI voltage controller and hysteresis current controller are implemented for both LED drive. As shown theses figures, a very low source current harmonics and high input power factor are achieved for the proposed LED driver.

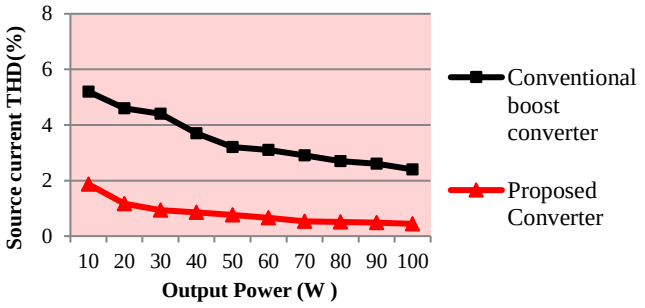

Fig. 16 a. Comparison of source current harmonics for conventional boost and proposed topology LED driver

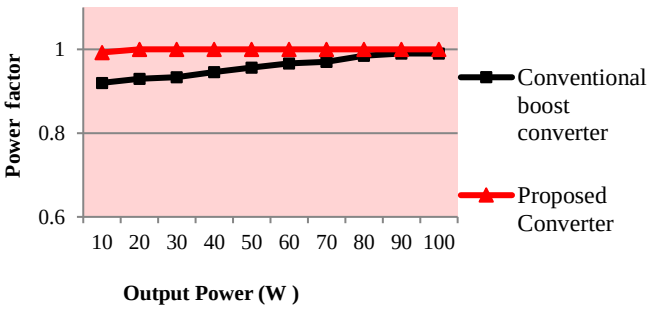

Fig. 16 b. Comparison of source side power factor for conventional boost and proposed topology LED driver

9. Conclusion

An improved power quality positive output super-lift Luo converter is proposed for high power LED industrial lighting applications. The proposed LED driver has shown high level performance such as low total harmonic distortion and unity power factor for variation of the LED lamp load power and variation of the supply voltage. From the simulation results, it is noted that the proposed driver with ANFIS tuned PI voltage and hysteresis current controller offers unsurpassed results with a very low THD of 0.44% with unity power factor at source side and on load side, the voltage is regulated with no peak overshoot, less settling time and rise time at load side under rated LED lamp load power. The ANFIS tuned PI voltage controller and the hysteresis current controller is implemented in a FPGA based hardware platform for proposed LED driver, with reduced input current THD of 1.24% in the experiment, along with the input power factor close to unity without any source side filter.

References

[1] H. J. Chiu and S. J. Cheng, IEEE Transaction on Industrial Electronics **5,** 2751(2007).
[2] H. Cho and O. K. Kwon, IEEE Transaction on Consumer Electronics **4,** 2054 (2010).
[3] C. S. Moo, Y. J. Chen, and W. C. Yang, IEEE Transaction on Power Electronics **11,** 4613 (2012).
[4] T. Hsieh, B. D. Liu, J. F. Wu, C. L. Fang, H. H. Tsai, Y. Z. Juang , IEEE Transactions on Power Electronics **12,** 4562 (2012).
[5] B. Lee, H. Kim, and C. Rim, IEEE Transactions on Power Electronics **26**, 3694 (2011).
[6] N. Chen, H. S. H. Chung, IEEE Transactions on Power Electronics **5,** 2551(2013).
[7] O. Faruk Farsakoglu, I. Atik, J. Optoelectron. Adv. M. **17,** 277(2015).
[8] An Tang, Yongtao Zhao, Haoming Zhang, Tao Ma, Fengxiang Shao, Hongsong Zhang, Optoelectron. Adv. Mat. **9**, 20 (2015).
[9] J. Liu, H. Yang, P. Jiang, M. Yu, Y. Huang, J. Yang, J. Optoelectron. Adv. M. **17**, 62 (2015).
[10] Wentao Zhang, Peicong Zhang, Junfeng Li, Kehui Qiu, Optoelectron. Adv. Mat. **8,** 37 (2014).
[11] Luqiao Yin, Jinlong Zhang, Yang Bai, Weiqiao Yang, Jianhua Zhang, Optoelectron. Adv. Mat. **8,** 427(2014).
[12] O. F. Farsakoglu, H. Y. Hasirci, J. Optoelectron. Adv. M.**17,** 816(2015).
[13] Jingquan Chen, Dragan Maksimovic, Robert W. Erickson, IEEE Transactions on Power Electronics **2,** 320 (2006).
[14] Bhim Singh, Ganesh Dutt Chaturvedi, Journal of Power Electronics, **4**, 318 (2007).
[15] Vashist Bist, Bhim Singh. IEEE Transaction on Industry Applications **2,** 871 (2015).
[16] J. M. Kwon, W. Y. Choi, J. J. Lee, E. H. Kim, B. H. Kwon, IEEE proceedings on Electronics Power Applications **5**, 673 (2006).
[17] Vashist Bist, Bhim Singh, IEEE Transactions on Industrial Informatics **4,** 2064 (2014).
[18] J. Gnanavadivel, N. Senthil Kumar, P. Yogalakshmi, J. Optoelectron. Adv. M. **18**, 459 (2106).
[19] Hung-Liang Chang, Ying-Nong Chang, Chun-An Chang, Chien-Hsuan Chang, Yu-Hung Lin, IET Power Electronics **9**, 2139(2016).
[20] H. Esam, Ismail, IEEE Transactions on Industrial Electronics **4**, 1147 (2009).
[21] Bhim Singh, Ambrish Chandra. IEEE Transactions on Industry Applications **51**, 1179 (2015).
[22] Y. He, F. L. Luo, IEEE Proceeding on Electric Power Application **152**, 1239 (2005).
[23] F. L. Luo, Electric power Applications, IEEE Proceedings on Electric power Applications**146**, 4415 (1999).
[24] F.L. Luo, IEEE Proceedings of the IEEE-PESC'98 / Fukuoka; Japan **22**, 1783 (1999).
[25] F. L. Luo, Proceedings of the second World Energy System international conference WES'98 Tornoto, Canada, 254 (1999).
[26] F. L. Luo, H. Ye, IEEE Transactions on Power Electronics **18**, 105 (2003).
[27] M. Zhu, F. L. Luo, Journal of Power Electronics**9**, 854 (2009).
[28] F. L. Luo, H, Ye, IEEE Transaction on Power Electronics, **18**,105 (2003).
[29] P. Comines, N. Munro, IEEE Proceeding Control Theory Application **149**, 46 (2002).
[30] G. L, Diego, F Arturo, A, Manuel, IEEE Transactionon Power Electronics **2**, 635(2008).
[31] K. H. C. Martin, H. L. C. Martin, K. T. Chi, IEEE Transaction on Industrial Electronics **2**, 665 (2008).
[32] R. Wu, S. B. Dewan, G. R. Slemon, IEEE Transactions on Industry Applications **26**, 880 (1990).
[33] W. C. So, C.K. Tse, Y. S, Lee, IEEE Transactions on Power Electronics **11**, 24 (1996).
[34] Y. P. Pan, J. E. Meng, D.P. Huang, Q.R. Wang, IEEE Transactions on Fuzzy Systems **5**, 807 (2011).
[35] R. K. Mudi, N. R, Pal, IEEE Transactions on Fuzzy Systems **1**, 2(1999).
[36] A. Al-Hmouz, J. Shen, R. Al-Hmouz, J. Yan, IEEE Transaction on Learning Technologies **5**, 226 (2012).
[37] K Premkumar, B. V. Manikandan,, Neurocomputing, **138**, 260 (2014).
[38] K. Premkumar, B. V, Manikandan, Neurocomputing, **157**, 76 (2015).

*Corresponding author: jgvadivel@gmail.com, gvadivel@mepcoeng.ac.in